Available online at www.sciencedirect.com
ScienceDirect
Energy Reports 6 (2020) 136–145
www.elsevier.com/locate/egyr

TMREES, EURACA, 04 to 06 September 2019, Athens, Greece

Multi-objective thermo-economic optimization of biomass retrofit for an existing solar organic Rankine cycle power plant based on NSGA-II

Joseph Oyekale[a,b,*], Mario Petrollese[a], Giorgio Cau[a]

[a] Department of Mechanical, Chemical and Materials Engineering, University of Cagliari, Via Marengo 2, 09123 Cagliari, Italy
[b] Department of Mechanical Engineering, Federal University of Petroleum Resources, Effurun, P.M.B. 1221 Effurun, Delta State, Nigeria

Received 19 September 2019; accepted 28 October 2019
Available online 5 November 2019

Abstract

Non-dominated sorting genetic algorithm (NSGA-II) was deployed in this paper for multi-objective thermo-economic optimization of biomass retrofit for an existing solar organic Rankine cycle (ORC) power plant. The existing plant consists of a field of linear Fresnel collectors (LFC), integrated directly with two-tank thermal energy storage (TES) system, which interfaces with ORC power block. The real solar-ORC plant currently runs at Ottana, Italy, albeit with some technical challenges basically due to inconsistent availability of solar irradiation. In order to upgrade the plant, a novel scheme had been proposed to install a biomass unit in parallel to the solar field, such that both LFC/TES and biomass furnace could directly and independently satisfy fractional thermal input requirement of the ORC. Being a retrofit system, existing design parameters of all the already operating units were imposed as equality constraints in this study, and the combustion excess air, as well as pinch point temperature difference of furnace heat exchangers that optimize the hybrid plant were investigated. Results showed that biomass mass flow rate of 0.133 kg/s and investment cost rate of 57 €/h are optimal for the studied biomass retrofit scheme. At this optimum point, excess air was obtained as 56%, furnace heater pinch point temperature difference as 28.8 ° C and air pre-heater pinch point temperature difference as 38.5 ° C. More generally, results showed that excess air value of less than 100%, furnace heater pinch point temperature difference of less than 80 ° C, and air pre-heater pinch point temperature difference of less than 80 ° C would optimize the studied biomass retrofit scheme.

Peer-review under responsibility of the scientific committee of the TMREES, EURACA, 2019.

Keywords: Solar-Biomass power plant; Organic Rankine cycle; Hybrid renewable energy; Multi-objective optimization; Non-dominated sorting genetic algorithm (NSGA-II); Power plant retrofit

1. Introduction

Universal campaign for de-carbonization of energy systems has been on drastic rise in recent years. Consequently, substantial financial and research efforts are growing tremendously, to enhance speedy development and practical

* Corresponding author at: Department of Mechanical Engineering, Federal University of Petroleum Resources, Effurun, P.M.B. 1221 Effurun, Delta State, Nigeria.
E-mail address: oyekale.oyetola@fupre.edu.ng (J. Oyekale).

https://doi.org/10.1016/j.egyr.2019.10.032

Peer-review under responsibility of the scientific committee of the TMREES, EURACA, 2019.

integration of renewable-based systems to modern energy architecture [1]. Amongst others, solar irradiation is one such renewable energy source that presently attracts huge investment in all fronts, and it is believed that market penetration of solar energy should be more vigorously pursued in the nearest future [2]. One major advantage of solar energy is that it is freely available for exploitation around the globe, and the cost to be incurred is limited to that of installation of exploitation and conversion facilities. However, solar-based energy infrastructures also possess major disadvantage of low system reliability, due majorly to transient nature of solar availability. Thus, this makes it extremely difficult for solar energy systems to follow scheduled profile of power supply and demand as it would be required in practice; efficiencies of available power conversion systems are quite low, and consequently, overall costs of energy production are extremely high. In order to ameliorate these attendant problems, a number of solution strategies are progressively under development, such as deployment of affordable energy storage systems, as well as hybridization of solar systems with more dispatchable renewable energy sources. Regarding the hybridization approach, geothermal and biomass energy sources are considered adequate [3]. But considering the capital intensity of drilling geothermal wells and special geological requirements of potential sites, the solar-biomass hybridization option could be considered more appropriate to address the aforementioned challenges of solar-only energy systems. Based on the foregoing, a lot of studies have examined different configurations of solar-biomass systems [4]. However, majority of the available studies considered series hybridization scheme, with focus on improvement of process parameters in new plant designs. With many solar-only systems already installed and operating around the world today, a need for biomass hybridization scheme that could be easily retrofitted to existing solar plants was recently realized, and this led to the proposal of a parallel scheme which could serve this purpose [5]. In particular, the proposed scheme was borne out of practical experience with a real concentrated solar power (CSP)-organic Rankine cycle (ORC) power plant which currently operates at Ottana, Italy [6]. Suffice it to mention that this paper further studied the aforementioned novel biomass retrofit for existing CSP-ORC plants, with main focus here being to investigate design parameters of the biomass furnace that would optimize thermo-economic performance of the fully-renewable hybrid energy plant post retrofit. The tangential objectives and contributions of this paper are:

- To obtain the Pareto frontier for maximum exergetic efficiency and minimum investment cost rate of the plant sequel to biomass hybridization;
- To determine optimal design parameters of the biomass retrofit system that satisfy the set dual objectives for the hybrid plant;
- To investigate the sensitivity of optimal design solutions to selected thermo-economic parameters.

2. Methodology

2.1. System description

The existing CSP-ORC plant being studied for potential upgrade has three main sections: the solar field section, the thermal energy storage (TES) section and the ORC section. The solar field is based on linear Fresnel collectors (LFC), using thermal oil as heat transfer fluid (HTF). The TES is directly coupled with the solar field, such that heated HTF is directly stored in the TES hot tank, from where the ORC is being fed. Also, the cold HTF exiting the ORC is stored in the TES cold tank, for circulation through the LFC. The same oil type (Therminol SP-I) is used as storage medium in the TES tanks as in the HTF circulating through the solar collectors. As power production unit, the recuperative ORC is of subcritical configuration, using hexamethyldisiloxane (MM) as working fluid. The accumulated thermal energy in the TES hot tank is transferred to the organic fluid through pre-heating and evaporating heat exchangers, while water is used as heat sink in the condenser.

For the biomass retrofit, a control-based modular furnace is positioned in parallel to the solar field, and connected to directly feed the ORC unit. The furnace is characterized by a combustion zone that is dominated by convection heat transfer processes, and separated from HTF heater (furnace heater). Hot combustion flue gases exiting the furnace heater preheat the inlet air into the combustion chamber, before escaping to the atmosphere. A three-way valve is placed upstream of the ORC, to regulate the flow of HTF from existing solar field and the retrofitted biomass furnace. For a close match with the existing system, the same HTF is considered in the biomass furnace heater as well. The complete scheme of both the existing CSP-ORC plant and the retrofitted biomass section is illustrated in Fig. 1. Comprehensive thermodynamic design of each section has been realized in a previous paper, including detailed thermo-economic analysis of the proposed biomass retrofit scheme [5]. For brevity, the design details are

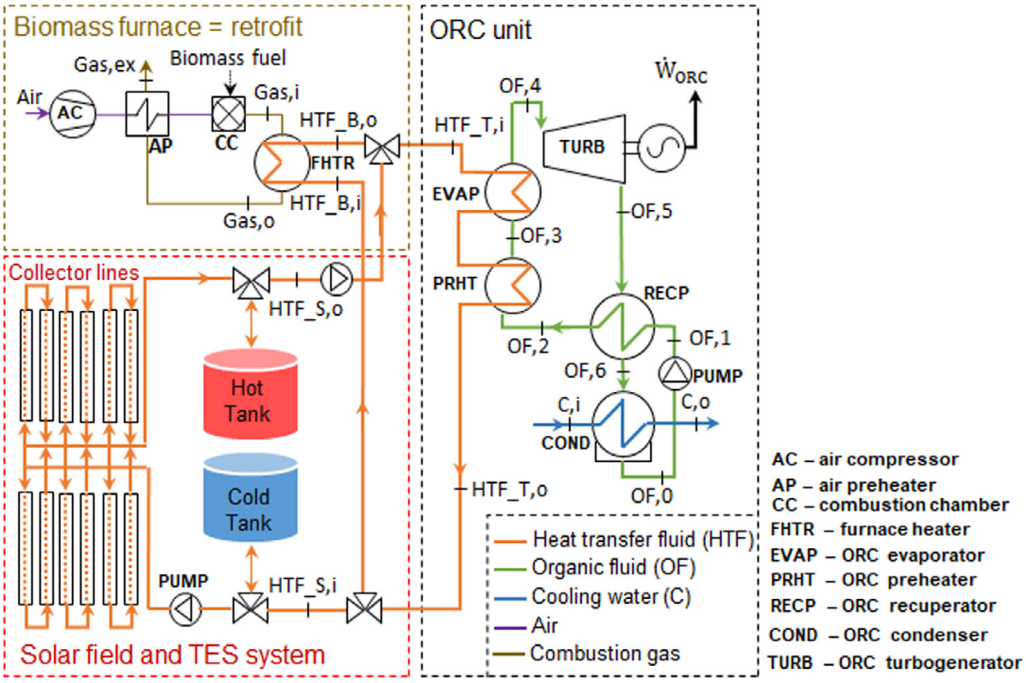

Fig. 1. Conceptual scheme of the hybrid CSP-biomass ORC plant [5].

not repeated in this paper, since the objective is to investigate the biomass retrofit that optimizes thermo-economic performance of the hybrid plant. However, detailed modeling approach adopted for the biomass system is essential to understand the optimization problem and is thus presented in the next section. The description of design parameters is given in Table 1.

Table 1. Design features of hybrid CSP-biomass ORC plant [5–7].

Existent CSP-ORC plant		Biomass furnace (retrofit)	
Design DNI	900 W/m^2	Furnace thermal duty	1430 kW
Solar field collecting area (A_{sf})	8400 m^2	Fuel composition (dry basis, % by weight)	48.3%C, 5.9%H, 0.1%N_2, 38.5%O_2, 7.2%Ash
Heat transfer fluid (HTF)	Therminol SP-I		
HTF inlet temperature ($T_{HTF,i}$)	165 °C		
HTF outlet temperature ($T_{HTF,o}$)	275 °C		
TES storage capacity	15.4 MWh		
ORC unit		LHV (dry basis)	16.3 MJ/kg
Net electrical power ($\dot{W}_{net}$)	629 kW	Moisture content	20%
Design thermal power input	3178 kW	Stoichiometric air–fuel ratio	5
Design HTF mass flow rate	11.05 kg/s	Combustion zone efficiency	99%

2.2. Retrofitted biomass furnace modeling

2.2.1. Combustion zone

The simulation of the biomass furnace requires estimation of the hot combustion gas temperature (T_{GAS}). The furnace mass and energy balance are given as follows:

$$\dot{m}_B + \dot{m}_{AIR} = \dot{m}_{GAS} + \dot{m}_{ASH} \tag{1}$$

$$LHV\,\eta_{FUR} = (\alpha + 1)\,(1 - y_{ASH})\,c_{P,GAS}\,(T_{GAS} - T_0) + y_{ASH} c_{ASH}\,(T_{GAS} - T_0) + y_{H20}\lambda_{H20} \tag{2}$$

where η_{FUR} is the combustion zone efficiency (related to convection and radiation losses to the environment), LHV is the lower heating value of biomass fuel, α is the ratio of air mass flow rate to ash-free biomass mass flow rate, y_{H20} is the water produced during the biomass combustion (without considering the biomass moisture), λ_{H20} is

the water evaporation heat (2.273 kJ/kg at ambient pressure), y_{ASH} is the ash content in the biomass (%weight), c_P represents specific heat capacity at constant pressure and T_0 is the ambient temperature. Thus, with known furnace efficiency and air–fuel ratio, it was possible to estimate gas temperature from the energy balance. The overall combustion reaction can be expressed by:

$$\begin{aligned} &C_m H_n O_x N_y S_z + x_W H_2O + \alpha_{St}(1+e)(wO_2 + yN_2 + zH_2O) \\ &\quad \rightarrow mCO_2 + (n/2 + x_W + \alpha_{St}(1+e)z)H_2O + (y/2 + \alpha_{St}(1+e)y)N_2 \\ &\quad + zSO_2 + (\alpha_{St}(1+e)w + x - m - n/4 - z)O_2 \end{aligned} \tag{3}$$

where α_{St} is the stoichiometric air–fuel ratio and e is the excess air (a decision variable in this study).

2.2.2. Boiler heat exchangers

A counter-flow heat exchanger was considered. By assuming the heat losses toward the environment negligible, the energy balance of the heat exchanger was used for calculating the required $\dot{m}_{GAS}$ under nominal conditions:

$$\dot{m}_{HTF}\left(h_{HTF,o} - h_{HTF,i}\right) = \dot{m}_{GAS}(h_{GAS} - h_{GAS,o}) \tag{4}$$

where $\dot{m}_{HTF}$ is the HTF mass flow rate, h is enthalpy, and subscripts i and o represent inlet and outlet, respectively. The HTF inlet and outlet temperatures were taken to coincide with exit and entry temperatures of the ORC at design conditions, and based on the thermal power required from biomass furnace, HTF mass flow rate was thus obtainable. The gas outlet temperature from furnace heater ($T_{GAS,o}$) relates with inlet HTF temperature ($T_{HTF,i}$) through furnace heater pinch point temperature difference ($\Delta T_{min,FHTR}$), which is a design variable in this study, as follows:

$$T_{GAS,o} = T_{HTF,i} + \Delta T_{min,FHTR} \tag{5}$$

Moreover, the required heat exchange area in the furnace heater (A_{FHTR}) was obtained from:

$$\dot{m}_{HTF}\left(h_{HTF,o} - h_{HTF,i}\right) = U_{FHTR} A_{FHTR} \Delta T_{ml,FHTR} \tag{6}$$

where U_{FHTR} is the overall heat transfer coefficient and $\Delta T_{ml,FHTR}$ is the mean logarithmic temperature difference. By assuming the conductive thermal resistance negligible, the overall heat transfer coefficient was obtained as:

$$U_{FHTR} = \frac{1}{\frac{1}{\gamma_{HTF,D}} + \frac{1}{\gamma_{GAS,D}}} \tag{7}$$

where $\gamma_{HTF,D}$ and $\gamma_{GAS,D}$ are the convective heat transfer coefficients under design conditions for the HTF and hot combustion gases, taken as 900 W/m^2 K and 150 W/m^2 K, respectively [8]. Similarly, temperature of pre-heated air ($T_{air,o}$) relates with $T_{GAS,o}$ through the air pre-heater pinch point temperature difference ($\Delta T_{min,AP}$), which is also a design variable, as follows:

$$T_{air,o} = T_{GAS,o} - \Delta T_{min,AP} \tag{8}$$

Consequently, the exchange area in the air pre-heater (A_{AP}) was calculated by using the correlation:

$$\dot{m}_{air} c_{P,air}\left(T_{air,o} - T_0\right) = U_{AP} A_{AP} \Delta T_{ml,AP} \tag{9}$$

where U_{AP} is the overall heat transfer coefficient of the air pre-heater, calculated according to Eq. (7) and by assuming convective heat transfer coefficient of air to be 150 W/m^2 K.

2.3. Optimization approach

The non-dominated sorting genetic algorithm (NSGA-II) multi-objective optimization approach proposed originally by Deb [9] was implemented in this study. The evolutionary algorithm possesses a number of highly desirable features, such as fast methodology for estimating crowding distance, relatively simple comparison operator for crowding, as well as speedy non-dominated sorting technique. Consequently, it is common to find this approach implemented in many detailed and recent optimization studies in literature [10–12].

In order to optimize thermo-economic performance of biomass retrofit for the existing CSP-ORC plant intended in this study, maximization of exergetic efficiency (ε) and minimization of investment cost rate ($\dot{C}$) were set as objective functions, defined as follows:

$$\varepsilon = \frac{\dot{W}_{net}}{\dot{E}_{sf} + (\dot{m}_B \cdot e_b)} \tag{10}$$

$$\dot{C} = \sum_k \mathrm{Z}_k \cdot \frac{1}{\mathrm{H}} \cdot \frac{i(1+i)^N}{(1+i)^N - 1} \cdot (1 + MF) \tag{11}$$

where $\dot{W}_{net}$ is the net electrical power produced by the power plant, $\dot{m}_B$ is the mass flow rate of biomass fuel, Z_k is the purchase and maintenance cost of component k, H is the number of annual operating hours of the plant (taken as 6000 h), MF is the maintenance factor (imposed equal to 6%), N is the lifetime of plant operation (assumed equal to 25 years) and i is the interest rate (taken as 7%). The exergy of solar irradiation entering the system ($\dot{E}_{sf}$) and specific exergy of biomass fuel (e_b) were obtained as follows [13,14]:

$$\dot{E}_{sf} = DNI \cdot A_{sf} \left[1 - \frac{4}{3}\frac{T_0}{T_s} + \frac{1}{3}\frac{{T_0}^4}{{T_s}^4}\right] \tag{12}$$

$$e_b = \beta \times LHV \tag{13}$$

where the direct normal irradiation (DNI), net effective area of solar collectors (A_{sf}), ambient temperature (T_0) and lower heating value (LHV) implemented are contained in Table 1. The temperature of the sun (T_s) was taken as 5770 K. For the exergy index of biomass fuel (β), model obtained from [14] was applied, as follows:

$$\beta = \frac{1.044 + 0.016\frac{H}{C} - 0.34493\frac{O}{C}(1 + 0.0531\frac{H}{C})}{1 - 0.4124\frac{O}{C}} \tag{14}$$

using the molecular weight of fuel elemental compositions specified in Table 1. Given that this study concerns a retrofit to a real and operational plant, design specifications of the existing units were preserved in the study being reported, thereby introducing equality optimization constraints for $\dot{W}_{net}$, $\dot{E}_{sf}$ as well as investment cost functions of the existing units. In essence, the main optimization variables lie with the newly introduced biomass furnace. Moreover, by imposing the aforementioned equality constraints, exergetic efficiency maximization would be satisfied by minimizing biomass consumption rate, based on Eq. (10). Therefore, the optimization problem is reduced to seeking design variables of main components of the biomass furnace that would minimize biomass mass flow rate and investment cost rate simultaneously, when retrofitted to the existing units. In more specific terms, combustion excess air supplied to the biomass furnace (e), pinch point temperature difference in the air pre-heater ($\Delta T_{min,AP}$) and pinch point temperature difference in the furnace heater ($\Delta T_{min,FHTR}$) were investigated for the multi-objective optimization problem studied in this paper, based on the relations expressed in Section 2.2 above. The lower and upper boundaries imposed for the optimized design variables were selected empirically, as highlighted in Table 2. Purchase cost relations were obtained from [15]. By optimizing $\Delta T_{min,FHTR}$ and $\Delta T_{min,AP}$, heat transfer processes in furnace heater and air pre-heater are improved, thereby reducing required surface areas and consequently purchase costs of the heat exchangers. Population size of 50 was implemented in the NSGA-II algorithm, with termination criterion set as 60 generations. The main optimization output is the Pareto frontier, which comprises optimal design variables for each population.

Table 2. Imposed values for optimization decision variables.

Parameter	Unit	Lower bound	Upper bound
Excess air	(%)	50	200
$\Delta \mathrm{T}_{\mathrm{min,FHTR}}$	°C	25	100
$\Delta \mathrm{T}_{\mathrm{min,AP}}$	°C	20	200

3. Results and discussion

3.1. Pareto frontier and optimized design variables

The solutions obtained for the studied optimization problem are presented as Pareto frontier, shown in Fig. 2. As aforementioned, the optimization scheme sought to minimize mass flow rate of biomass consumed by the hybrid

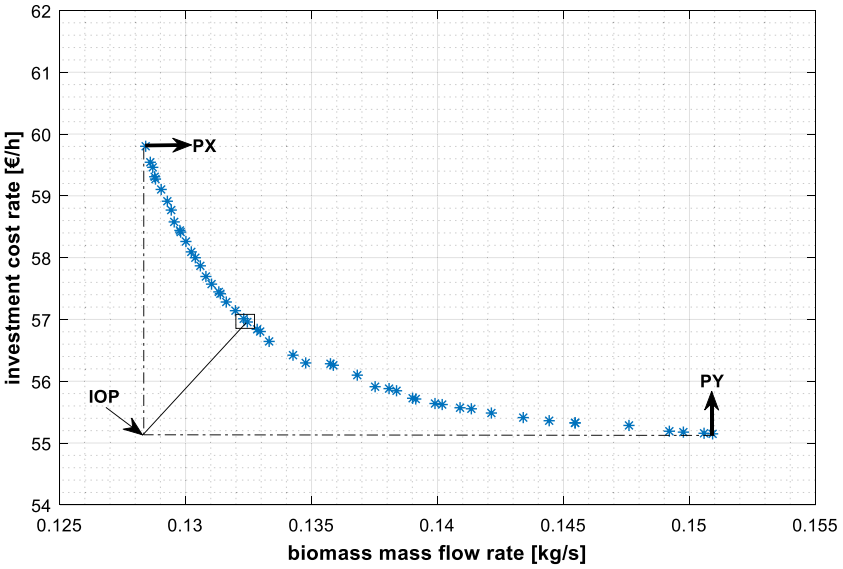

Fig. 2. Pareto frontier of the optimized biomass retrofit.

plant (with the original intention of maximizing exergy efficiency of the overall hybrid plant), while also minimizing investment cost rate of the hybrid plant. It should first be pointed out that each solution point shown in Fig. 2 could give optimal biomass retrofit to the existing solar-ORC plant. Any of the solution points could be selected by the designer, based on empirical and/or technical criteria. As it can be confirmed from Fig. 2, the solution points that minimize biomass mass flow rate also maximize investment cost rate, and vice versa, giving conflicting effects to the set objectives. Exemplarily for the conflicting effects, increasing pinch point temperature differences of heat exchangers lower required heat exchange surface areas, in favor of cost objective function, but it also lowers exergetic efficiency, against thermodynamic objective function. However, reduction in biomass mass flow rate from 0.150 kg/s to about 0.135 kg/s increases investment cost rate of the hybrid plant only marginally, while further reduction in biomass mass flow rate leads to more significant increase in investment cost rate. This signals the fact that the optimum solution lies around biomass flow rate of 0.135 kg/s. More specifically, this assertion was confirmed by another decision-making analysis. The minimum mass flow rate represented in Fig. 2 corresponds to point PX, and it is the best solution that satisfies the single objective of minimizing biomass mass flow rate. Conversely, the minimum investment cost rate corresponds to point PY in Fig. 2, and it is also the best solution that satisfies single objective of minimizing investment cost rate of the hybrid solar-biomass power plant. By drawing a straight line towards horizontal axis from PX and a straight line towards vertical axis from PY, an intersection point of the straight lines is obtained, termed here as imaginary optimal point (IOP). At IOP, the two optimization objectives are well satisfied, and it would ordinarily provide the best design. However, this point is out of the Pareto frontier, and it cannot provide real solution to the multi-objective optimization problem. In this regard, the next best solution is to be selected, which is the point on the Pareto frontier that is closest to IOP. The selected optimal design point is boxed in Fig. 2, with biomass mass flow rate and investment cost rate of about 0.133 kg/s and 57 €/h, respectively. The design variables at the selected optimal point, as well as those satisfying individual single objectives (points PX and PY), are highlighted in Table 3. In addition, positions of $\Delta T_{min,FHTR}$ and $\Delta T_{min,AP}$ are

Table 3. Design variables at single and selected multi-objective optimal points.

Point	Excess air (%)	$\Delta T_{min,FHTR}$ (°C)	$\Delta T_{min,AP}$ (°C)
PX	153	25.9	20
PY	50	77.3	123.5
Multi-objective choice	56	28.8	38.5

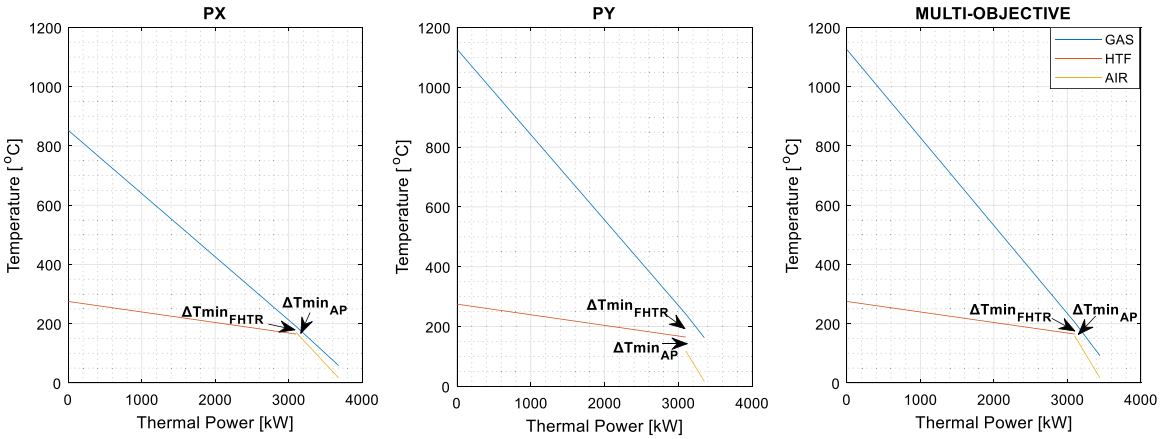

Fig. 3. Heat exchange characteristics in the biomass boiler for different optimization solution points.

illustrated by heat-exchange characteristic diagram, for the three optimization solution points, as shown in Fig. 3. Furthermore, design variables that produced each optimized solution on the Pareto frontier are represented in form of scatter distribution, as shown in Fig. 4. Specifically, distributions of excess air, pinch point temperature difference of furnace heater as well as pinch point temperature difference of air pre-heater on the Pareto frontier are illustrated in Fig. 4a–c, respectively.

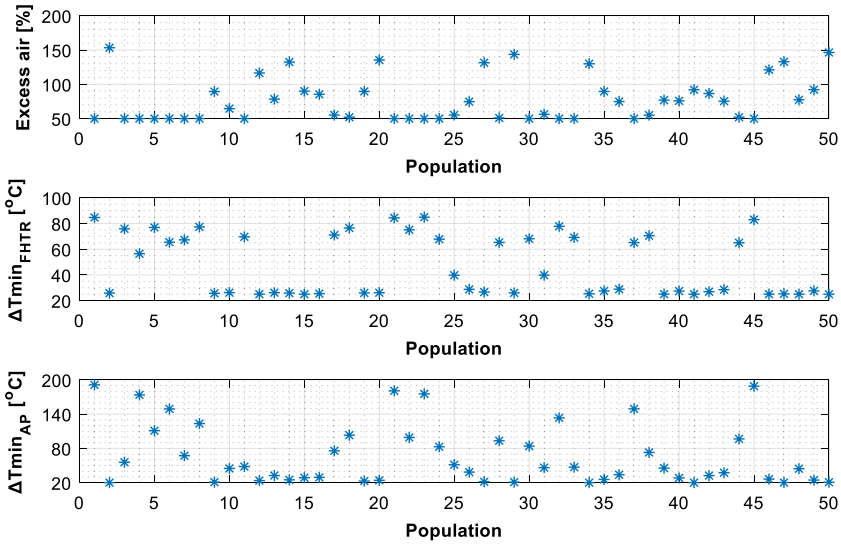

Fig. 4. Scatter distribution of design variables at Pareto frontier.

As it can be seen, about 80% of solution points on the Pareto frontier have their excess air value between 50% and 100%. The implication of this is that the desired excess air value that satisfies the dual-objective optimization problem investigated in this paper is less than 100%. This contradicts the insinuation that high excess air of 153% optimizes the thermodynamic performance of the biomass retrofit, as obtained in point PX and Table 3 for single objective optimization. The importance of such multi-objective optimization as studied in this paper is thus underscored. Also, it is observed in Fig. 4b that values of pinch point temperature difference of furnace heater on Pareto frontier are evenly distributed, with highest density observed between 20 and 80 °C, making it the preferred range. Similarly, Fig. 4c shows that about 60% of values of pinch point temperature difference for air pre-heater on the Pareto frontier are between 20 and 80 °C, which makes the desired value for the dual-objective optimization to fall within this range.

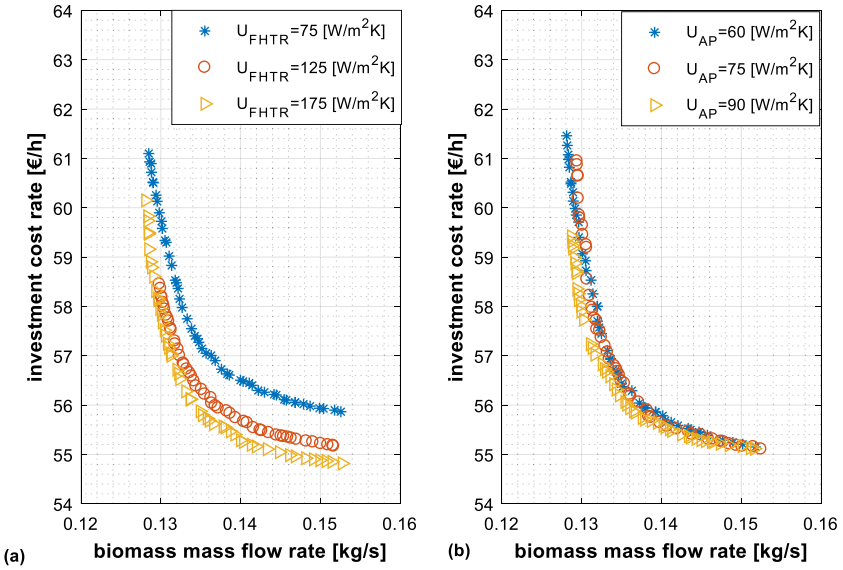

Fig. 5. Sensitivity of optimal solutions to heat exchanger overall heat transfer coefficient.

3.2. Sensitivity analyses

Either due to imperfect design or inevitable variation of adopted design parameters during actual operation, real-time workings of energy systems often deviate from predictions at design conditions. It is thus a good practice to evaluate performance of system designs with changes in selected design parameters. In this paper, sensitivity of the obtained optimal solutions to both thermodynamic and economic parameters have been investigated. In particular, Fig. 5 shows the behavior of Pareto frontier with change in overall heat transfer coefficient of furnace heater (U_{FHTR}) and air pre-heater (U_{AP}). As it would be expected, increasing U_{FHTR} shifts the Pareto frontier downwards, thereby reducing investment cost rate at optimal points, albeit with marginal increase in biomass mass flow rate. It is however worthwhile to note that the downward shift in the optimal solutions is less significant with U_{FHTR} of more than 125 W/m^2 K, relative to lower values. A similar effect is obtained for air pre-heater, however with less absolute significance. The reason for this is obvious; enhancing heat transfer performance of an heat exchanger reduces required surface area, and consequently the investment cost. In addition, Fig. 6 shows the sensitivity of the optimal solutions to interest rate value (i) and annual operating hour of the plant (H). Similar patterns are observed in the Pareto frontier for all interest rates implemented, with optimal solutions shifting upwards as interest rate increases, as expected. Moreso, increase in annual operating hours of the hybrid plant shifts the Pareto frontier downwards, due to consequent reduction in investment cost rates. In essence, the clamour for hybridization of transient renewable energy sources such as solar and wind to enhance dispatchability and annual operating hours is justified.

4. Conclusions

Biomass retrofit for an existing CSP-ORC power plant has been optimized thermo-economically in this study, based on the multi-objective NSGA-II evolutionary approach. Design parameters of the currently operating units were adopted as equality constraints in the optimization problem, leaving the possible optimization decision variables to biomass furnace parameters. In particular, the combustion excess air value, as well as pinch point temperature difference of the air pre-heater and furnace heater were set as decision variables. The objective was to simultaneously minimize biomass consumption rate (equivalent to maximizing exergetic efficiency of the retrofitted hybrid plant at nominal conditions) as well as investment cost rate of the hybrid plant post retrofit. The main findings are highlighted below:

- Amongst several possible optimal solutions represented by the Pareto frontier, the design point with biomass mass flow rate of about 0.133 kg/s and investment cost rate of about 57 €/h was adjudged the most adequate

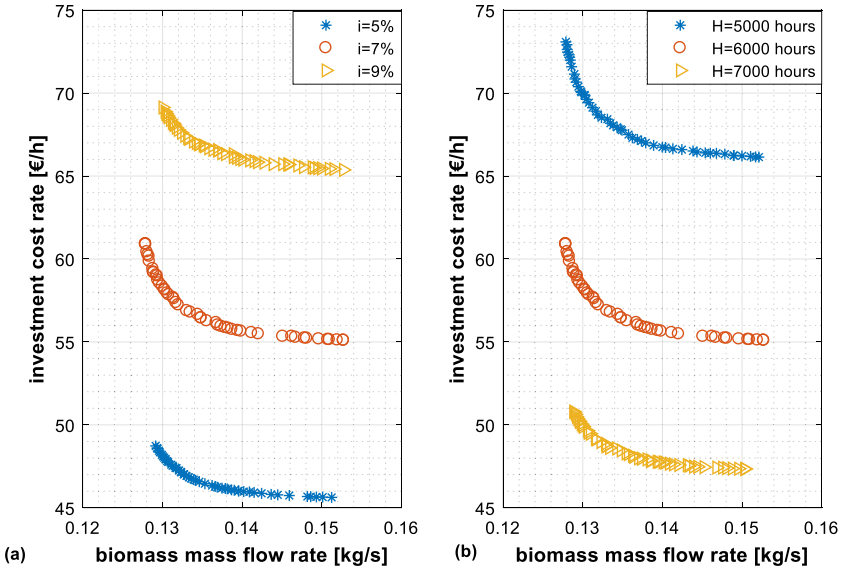

Fig. 6. Sensitivity of optimal solutions to interest rate (i) and annual operating hours (H).

for the studied biomass retrofit. At this point, excess air was obtained as 56%, furnace heater pinch point temperature difference as 28.8 °C and air pre-heater pinch point temperature difference as 38.5 °C.

- For the optimization of biomass retrofit studied in this paper, excess air value of less than 100%, furnace heater pinch point temperature difference of less than 80 °C, and air pre-heater pinch point temperature difference of less than 80 °C were found to satisfy the set objectives the most.
- Lower investment cost rate would be achieved for the hybrid plant post biomass retrofit, with lower interest rate and peradventure the hybrid plant operates for longer hours annually. Also, the optimal design solutions for biomass retrofit reported in this study are less sensitive to furnace heater overall heat transfer coefficient higher than 125 W/m^2 K, as well as for the range implemented for the air pre-heater in this study (75 W/m^2 K).

Acknowledgments

This study was carried out under the Cooperation Agreement with “Ente Acque Sardegna” (ENAS) for the realization of the project “Thermodynamic solar plant for the development of an electrical and thermal energy smart grid” funded by P.O.R FESR, Italy 2014 – 2020 – Action line 4.3.1 – Framework agreement PT_CRP “Su Suercone Ambiente Identitario”.

The authors thank ENAS for providing operational data and information on the Ottana Solar Facility and for setting up the experimental ORC plant.

References

[1] Sim J. The economic and environmental values of the R&D investment in a renewable energy sector in South Korea. J Clean Prod 2018;189:297–306. http://dx.doi.org/10.1016/J.JCLEPRO.2018.04.074.

[2] Stević I, Mirjanić D, Stević S. Possibilities for wider investment in solar energy implementation. Energy 2019;180:495–510. http://dx.doi.org/10.1016/J.ENERGY.2019.04.194.

[3] Pramanik S, Ravikrishna RV. A review of concentrated solar power hybrid technologies. Appl Therm Eng 2017;127:602–37. http://dx.doi.org/10.1016/J.APPLTHERMALENG.2017.08.038.

[4] Hussain CMI, Norton B, Duffy A. Technological assessment of different solar-biomass systems for hybrid power generation in europe. Renew Sustain Energy Rev 2017;68:1115–29. http://dx.doi.org/10.1016/j.rser.2016.08.016.

[5] Oyekale J, Heberle F, Petrollese M, Brüggemann D, Cau G. Biomass retrofit for existing solar organic rankine cycle power plants: Conceptual hybridization strategy and techno-economic assessment. Energy Convers Manag 2019;196:831–45. http://dx.doi.org/10.1016/j.enconman.2019.06.064.

[6] Petrollese M, Cau G, Cocco D. The ottana solar facility: dispatchable power from small-scale CSP plants based on ORC systems. Renew Energy 2018. http://dx.doi.org/10.1016/j.renene.2018.07.013.

[7] Mureddu M, Dessì F, Orsini A, Ferrara F, Pettinau A. Air- and oxygen-blown characterization of coal and biomass by thermogravimetric analysis. Fuel 2018;212:626–37. http://dx.doi.org/10.1016/j.fuel.2017.10.005.
[8] Shah RK, Sekulić DP. Fundamentals of heat exchanger design - Shah - Wiley Online Library. John Wiley & Sons, Inc; 2007, http://dx.doi.org/10.1002/9780470172605.
[9] Deb K. NSGA II Paper by kalyanmoy deb. 182. IEEE Trans Evol Comput 2002;6:182–97. http://dx.doi.org/10.1109/4235.996017.
[10] Niu X, Wang H, Hu S, Yang C, Wang Y. Multi-objective online optimization of a marine diesel engine using NSGA-II coupled with enhancing trained support vector machine. Appl Therm Eng 2018;137:218–27. http://dx.doi.org/10.1016/J.APPLTHERMALENG.2018.03.080.
[11] Wang S, Zhao D, Yuan J, Li H, Gao Y. Application of NSGA-II algorithm for fault diagnosis in power system. Electr Power Syst Res 2019;175:105893. http://dx.doi.org/10.1016/J.EPSR.2019.105893.
[12] Yan F, Wei L, Hu J, Zeng J, Zheng S, Wang J. Simultaneous optimization of urea dosing and ammonia coverage ratio of selective catalytic reduction system in diesel engine by using physico-chemical model based NSGA-II algorithm. Appl Therm Eng 2019;154:46–62. http://dx.doi.org/10.1016/J.APPLTHERMALENG.2019.03.031.
[13] Petela R. Exergy of heat radiation. J Heat Transfer 2012;86(187). http://dx.doi.org/10.1115/1.3687092.
[14] Kotas TJ. The exergy method of thermal plant analysis. Butterworths; 1985.
[15] Turton R, Bailie RC, Whiting WB, Shaeiwitz JA, Bhattacharyya D. Analysis, synthesis, and design of chemical processes. fourth ed.. Upper Saddle River, NJ (USA): Prentice Hall; 2012.